Proceedings of the 16th International Conference on Soil Mechanics and Geotechnical Engineering

doi:10.3233/978-1-61499-656-9-2511

Evaluation of shear strength parameters for rain-induced slope instabilities

Evaluation des paramètres de résistance au cisaillement pour des instabilités de pentes induites par des précipitations

Khalid Farooq
University of Engineering and Technology, Lahore, Pakistan

Rolando P. Orense
Chuo Kaihatsu Corporation, Tokyo, Japan

Ikuo Towhata
University of Tokyo, Tokyo, Japan

ABSTRACT

The stress path followed by a soil element along a potential failure plane in a slope subjected to rainfall infiltration is characterized by pore pressure increase at almost constant total stress condition. This stress path can be simulated in the laboratory by conducting constant shear stress drained (CSD) triaxial tests wherein back pressure within a saturated soil specimen is increased while keeping the shear stress constant, i.e. σ_1 and σ_3 are kept constant. Such stress path is obviously different from that reproduced in conventional triaxial tests in which σ_3 remains constant and σ_1 increases. To investigate the soil response under different stress paths, CSD tests, as well as conventional triaxial drained and undrained tests, were performed on sandy soils obtained at previous landslide sites. The test results confirmed that CSD-derived strength parameters were more appropriate when analyzing rainfall-induced failure initiation. Realizing that CSD tests are not easy to perform, correlations were made to express the strength parameters obtained through conventional triaxial tests with those derived from CSD tests.

RÉSUMÉ

L'évolution des efforts subis par un élément de sol sur un potentiel plan de rupture dans une pente soumise à des infiltrations lors de précipitations est caractérisé par une augmentation de la pression dans les pores avec des efforts globaux presque constants. Cette évolution peut être simulée en laboratoire en conduisant des essais triaxiaux drainés avec effort de cisaillement constant (CSD) dans lesquels la contre-pression dans le specimen de sol saturé est augmentée en gardant l'effort de cisaillement constant, c'est -à-dire σ_1 et σ_3 constants. Une telle évolution des efforts est sans aucun doute différente de celle produite lors des tests triaxiaux conventionnels où σ_3 est constant alors que σ_1 augmente. Pour étudier la réponse du sol sous différentes évolutions des efforts, des tests CSD et des tests conventionnels drainés et non-drainés ont été realisés sur des sols sableux récupérés sur des sites ayant auparavant subis des glissements de terrain. Les résultats de ces tests confirment que les paramètres de force que l'on retire des tests CSD sont plus appropriés pour analyser l'initiation d'une rupture de pente induite par des précipitations. Réalisant que ces tests CSD ne sont pas aisés à mettre en oeuvre, des correlations sont recherchées pour exprimer les paramètres de force obtenus par des tests conventionnaux à partir de ceux obtenus lors des tests CSD.

1 INTRODUCTION

Stability analysis of natural or man-made slopes subject to rainwater infiltration often employs strength parameters derived from saturated conditions using conventional testing procedures. However, the stress changes which a soil element undergoes in rain-induced slope failure are quite different from those typically reproduced in conventional laboratory tests. Moreover, since rain-induced landslides generally occur in steep and marginally stable slopes, it follows that initial stress state is closer to failure state and that relatively small disturbance can initiate failure.

To fully understand the deformation characteristics of soil slopes under rainwater infiltration, it is important to simulate real in-situ condition in laboratory tests. As pointed out by various researchers (Brand, 1981; Brenner et al., 1985), this can be achieved through constant shear stress drained (CSD) tests, wherein total normal stress, σ, and shear stress, τ, essentially remain constant during infiltration.

To simulate actual condition, CSD tests were conducted on fully saturated soil samples obtained from former landslide sites by increasing pore-water pressure within the specimen until failure occurs. Since this type of test is rather specialized, the difference in soil response between this test and conventional triaxial tests was examined. Finally, the implications of the test results on slope stability problem under rainfall condition were addressed, with emphasis on appropriate shear strength parameters to be used in analyzing slope instability.

2 IN-SITU AND LABORATORY STRESS PATHS

During rainwater infiltration, soil element along a potential failure plane follows a stress path which is characterized by gradual increase in pore-water pressure while total normal stress, σ, and shear stress, τ, on the element remain essentially constant. This is different from the stress paths followed in conventional triaxial tests, which involve increasing σ_1 while maintaining constant σ_3. Figure 1 compares the stress paths normally followed in standard triaxial tests (i.e., consolidated undrained (CU) and consolidated drained (CD) tests) and the path which reflects field condition during rainfall.

This difference in stress paths further implies that the ranges of stress over which conventional triaxial tests are usually conducted may not be appropriate to what is actually happening in the field during rainfall. Slope failures are typically shallow and, therefore, in-situ stresses are generally lower than those normally applied in conventional triaxial compression tests. In order to obtain meaningful shear properties from laboratory tests for the analysis and design of slopes subjected to rainwater infiltration, it is essential when conducting laboratory tests to simulate as close as possible the stress path in the field.

In this paper, typical results of CSD tests are discussed in relation to those obtained from conventional tests. Comparison of strength parameters obtained from different stress paths, such as anisotropically consolidated drained (ACD) and undrained (ACU) tests and isotropically consolidated drained (ICU) tests, are also presented.

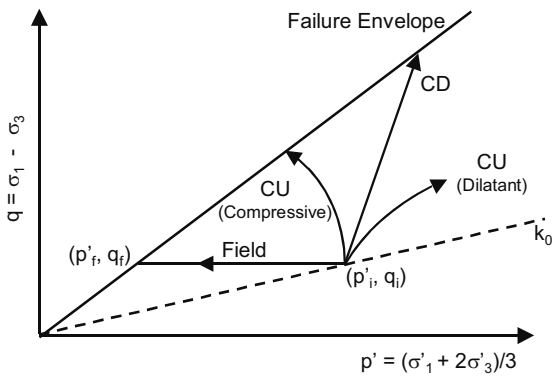

Figure 1. Comparison between field and laboratory-reproduced stress paths. CU refers to consolidated undrained tests while CD denotes consolidated drained tests.

3 MATERIALS, APPARATUS AND TEST PROCEDURE

The materials used were sampled from two natural slopes in Japan where landslides due to rainfall occurred in the past. Two sets of samples were taken in a natural slope in Kumanodaira, Gunma Prefecture, where a series of large-scale landslides occurred in 1950. The sample obtained from upper part of the slope was gravelly sand (hereafter Kumano-gravelly sand), while the one obtained in the lower portion was silty sand (hereafter Kumano-silty sand). The third sample (Omigawa sand) was obtained in Omigawa, Chiba Prefecture, site of more than 250 rain-induced landslides in 1971. Grain size distribution curves of these three soil types are shown in Figure 2.

In laboratory tests, a conventional stress-controlled triaxial test apparatus was modified to allow shearing infiltration tests to be conducted. In the system, axial stress, cell pressure, and pore-water pressure can be independently controlled through electro-pneumatic transducers. Volume change was measured through a burette while axial strain was monitored by a linear variable differential transducer.

The soil specimen, 155 mm high and diameter of 75 mm, was prepared by wet tamping method to obtain a predetermined relative density, *Dr*. To saturate the sample, a confining pressure of 20 kPa was applied to the specimen and CO_2 was circulated for about 2 hrs, followed by flushing with de-aired water. Back-pressure was then applied to obtain *B*-values > 0.96 for all the tests. After confirming full saturation, the specimen was first isotropically, and if necessary, anisotropically consolidated to the specified level of principal stress ratio ($K=\sigma'_1/\sigma'_3$). After consolidation, the specimen was sheared according to the prescribed stress path.

In CSD tests, the specimen was brought to failure by gradually increasing the back-pressure within the specimen through an electro-pneumatic controller while maintaining axial and radial stresses constant. In conducting conventional triaxial tests, such as ICD, ACD and ACU tests, specimens under the same initial conditions as those of CSD tests were sheared in conventional manner, i.e. σ_3 remained constant and σ_1 was increased, with drainage valve either opened or closed, depending on whether the tests are drained or undrained, respectively.

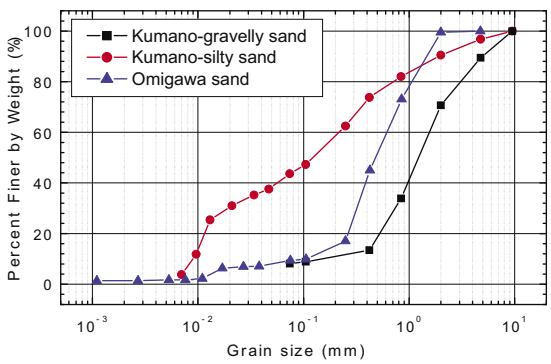

Figure 2: Grain size distribution curves of test materials

4 TEST RESULTS AND DISCUSSIONS

The effects of various parameters, such as initial relative density (*Dr*), initial principal stress ratio, K ($=\sigma'_1/\sigma'_3$), rate of pore water pressure increase, *r*, and initial confining pressure, σ'_3, on the development of failure in the initially saturated specimen were examined. Due to space limitation, only limited test results are discussed herein. Other test results are presented elsewhere (Farooq, 2002).

Figure 3 shows the results of CSD tests on Kumano-silty sand wherein initial conditions of K=1.4 and σ'_3=25 kPa were kept constant, and relative density was varied from *Dr*=58~83%. As shown in Figure 3(a), the increase in pore-water pressure during the initial phase of the test did not cause any significant increase in axial strain of the specimen. However, after a certain level of pore-water pressure had developed, failure started to occur in the specimen and axial strain developed rapidly. As shown in Figure 3(b), the compressive volume change of the specimen after failure initiation (denoted by Δ in the figure) caused sudden build-up of pore-water pressure, resulting in rapid failure. Thus, undrained condition prevailed within the specimen during the deformation mode which caused the pore-water pressure to increase.

Similar behavior of almost zero axial strain during the initial phase of the test was also observed in Kumano-gravelly sand and in Omigawa sand (Farooq, 2002). However, once failure was induced in these soils, the deformation mode was generally dilative. In these cases, dilation accompanying the deformation process caused a decrease in pore-water pressure and an increase in soil resistance, resulting in slower failure.

Figure 4(a) shows the changes in stress state of all Kumano-gravelly sand samples in the void ratio (*e*) ~ stress (*p'*) space.

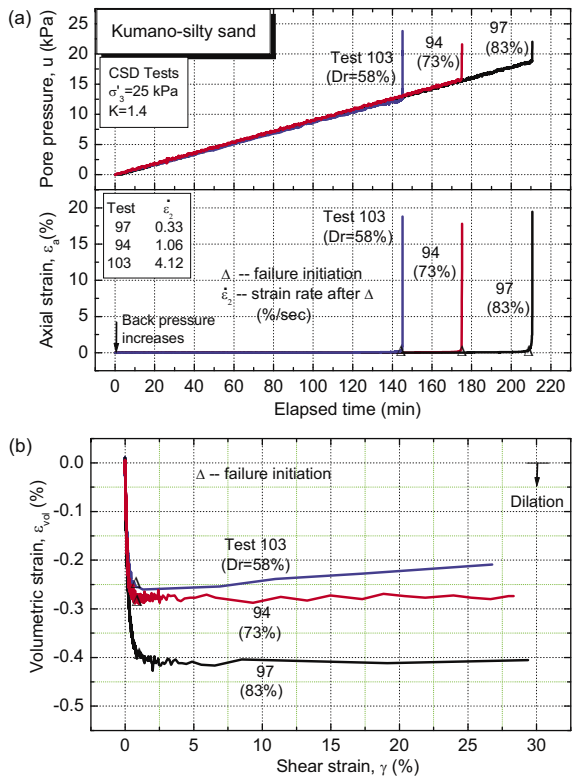

Figure 3: Time histories of (a) axial strain, ε_a, over-all degree of saturation, *Sr*; (b) pore water pressure, *u*, showing the effect of initial relative density, *Dr* on Kumano-silty sand

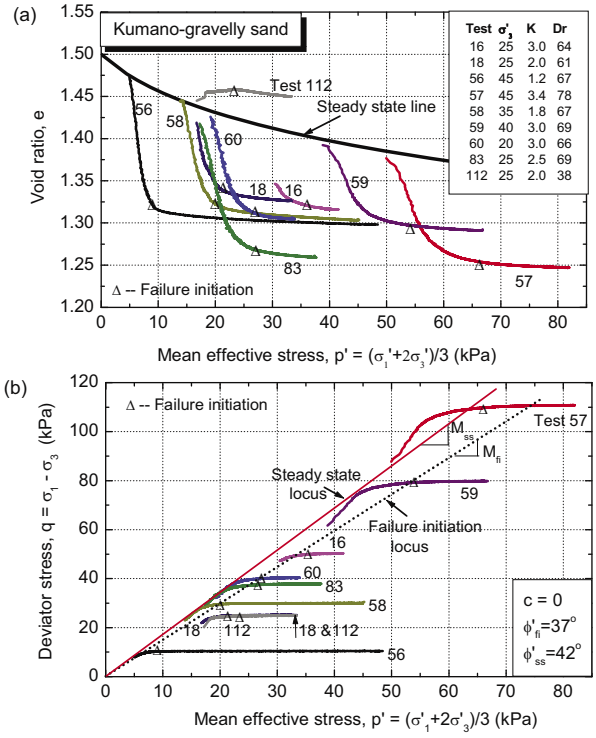

Figure 4, Summary of CSD test results for Kumano-gravelly sand: (a) $e \sim p'$ relation and estimated steady state line; (b) stress paths

When a sample is sheared to large level of axial strain (>15%), it is reasonable to assume that it is at steady state at the end of the test (Fell et al., 2000). Steady state is the condition where a sample continues to deform with no change of state, i.e., constant shear stress, normal stress and void ratio. With this assumption, the locus of points defining the steady state condition for all samples under different initial conditions, called the steady state line, is obtained by linear-log fit. For Kumano-gravelly sand, all test results plot below the steady state line and show dilative response, except for Test 112 (lowest *Dr*) which plots above the steady state line and shows compressive behavior. The steady state line therefore is useful in identifying possible volume change behavior of in-situ soil subjected to field stress path during rainfall. If the state of soil in $e \sim p'$ space at failure initiation is above the steady state line, the soil behavior is compressive and this can give rise to development of pore-water pressure during deformation and can result in rapid failure. Conversely, if the state of soil at failure initiation is below the said line, the volumetric behavior is dilative and soil can undergo slower movement due to decrease in pore pressure associated with shearing process.

The stress paths followed by soil in p'~q space are essentially horizontal, as shown in Figure 4(b). However, when failure starts, a drop in shear stress occurs as a result of increase in cross-sectional area of the specimen associated with increase in radial strain. At the end of the test, the specimens are assumed to be at steady state of deformation. Condition of failure initiation for each test can be represented by a line with slope M_{fi}, as shown in the figure. Similarly, the locus of points defining the steady state condition can be identified by a line with slope M_{ss}. Thus, the friction angle, ϕ', associated with these conditions can be calculated from the appropriate slope M, i.e.,

$$\varphi' = \sin^{-1}\frac{3M}{6+M} \tag{1}$$

Friction angles obtained for Kumano-gravelly sand corresponding to failure initiation and steady state conditions are indicated in Figure 4(b). Note that both lines pass through the origin, indicating zero cohesion. Values of shear strength

Table 1: Friction angles calculated from different stress paths

Soil type	CSD		ICD	ACD	ACU	
	ϕ'_{ss}	ϕ'_{fi}	ϕ'_{pk}	ϕ'_{pk}	ϕ'_{ss}	ϕ'_{pk}
Kumano-gravelly sand	42	37	43	-	-	-
Kumano-silty sand	37	30	38	-	37	29
Omigawa sand	34	27	36	35	34	26

Note: The subscripts *ss*, *pk* and *fi* refer to steady state, peak state and failure initiation conditions, respectively

parameters for the three soil types derived by CSD tests are summarized in Table 1.

To illustrate the behavior of soil subjected to different stress paths, CSD and ACD tests were conducted on several sets of Omigawa sand specimens under essentially similar initial conditions. Results are summarized in Figure 5, where appropriate conditions are indicated. Stress paths are shown in Figure 5(a) while strain paths are indicated in Figure 5(b). Notice the completely different response of these two sets. In CSD tests, shearing is performed through water infiltration, which reduces the effective confinement of specimen. As a result, the soil grains are pushed out leading to significant radial strains and more dilative behavior. In ACD tests, on the other hand, shearing is due to continuous increase in shear stress, and axial strain is more predominant; hence soil behavior is compressive. Note that increasing K in CSD tests makes the soil behavior less dilative, while ACD tests show the opposite.

Friction angles for the three samples corresponding to various stress paths and conditions are also summarized in Table 1.

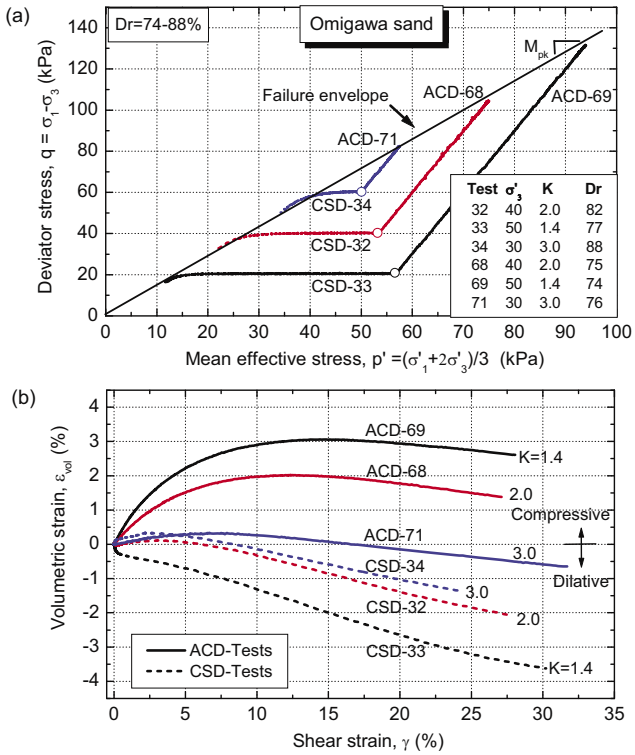

Figure 5. Comparison of ACD and CSD test results for Omigawa sand: (a) stress paths; (b) strain paths

5 STEADY STATE UNDER DIFFERENT STRESS PATHS

Since the tests under different stress paths were conducted using a stress-controlled apparatus, it was not possible to observe the steady state in all cases. However, because all tests were continued until large deformation range (ε_a >15%), it is reasonable to assume that samples at the end of test are at steady state condition (Anderson and Sitar, 1995; Fell et al., 2000).

Figure 6 summarizes the steady state conditions in p'~q space of the three soil types under different stress paths. In each figure, all points corresponding to steady state condition almost lie on a straight line irrespective of the stress path. This indicates that the specimens, at least those within the range of *Dr* specified in each figure, reached the same steady state line at the end of tests. The strength parameters corresponding to steady state (φ'_{ss}) are indicated in the figures. Thus, steady state strength parameters of a particular soil can be considered to be unique even if stress paths are different. This observation is reflected in Table 1, which summarizes the friction angles calculated for each soil type under different stress paths.

Also shown in respective plots in Figure 6 are lines defining failure initiation in CSD tests for each soil type and strength parameters associated with this condition (φ'_{fi}). These parameters are generally lower than those at steady state and their relations indicated at the bottom of each figure.

6 IMPLICATIONS ON SLOPE STABILITY ANALYSIS

Based on test results presented here, CSD test is more accurate in reproducing the stress path followed by soil elements in-situ, as compared to conventional triaxial tests. Hence, in determining strength parameters for slope stability analyses under rainfall condition, it would be more appropriate to use laboratory test results based on CSD condition. A good indicator of the critical condition is when a soil element reaches its yield strength during water infiltration and large deformation commences, i.e., the failure initiation point.

Since CSD tests are not very simple to perform, friction angle at failure initiation can be estimated based on test results which show that the steady state is unique for different stress paths. From Figure 6, the friction angle corresponding to failure initiation in CSD tests, φ'_{fi} , is related to the friction angle associated with the steady state of soil, φ'_{ss} , in the form

$$\tan\varphi'_{fi} = 0.73 \sim 0.83 \tan\varphi'_{ss} \qquad (2)$$

Note that the factor relating the two angles is, in general, a function of type and state of soil (fines contents, mean grain size, relative density, etc.). For more accurate relation considering various soil types, more tests are recommended.

Therefore, instead of performing complicated CSD tests, any conventional drained or undrained triaxial test can be conducted on soil specimens until steady state condition is reached. Then, by using Equation (2), appropriate value of friction angle to be used in analyzing failure initiation in sandy slopes caused by rainwater infiltration can be estimated. Note that since lower strength parameters are associated with failure initiation state as compared to peak or residual (steady state) condition, lower values of factor of safety can be obtained when performing stability analysis, resulting in more conservative estimate of slope stability under rainwater infiltration.

7 CONCLUSION

Triaxial tests performed on three different sandy materials revealed that CSD tests are more accurate in reproducing the in-situ behavior of soil elements during rainfall, as compared to conventional triaxial tests. Consequently, strength parameters associated with failure initiation in CSD tests are more appropriate in analyzing slope stability due to rainfall. Since irrespective of the stress path, steady state conditions were found to be almost unique for a particular soil type, friction angle mobilized at failure initiation state, φ'_{fi} , can be related to friction angle at steady state, φ'_{ss} . Hence, by performing any conventional drained or undrained triaxial test on sample specimen until steady state condition is reached, the appropriate value of friction angle to be used in analyzing failure initiation in sandy slopes caused by rainwater infiltration can be estimated.

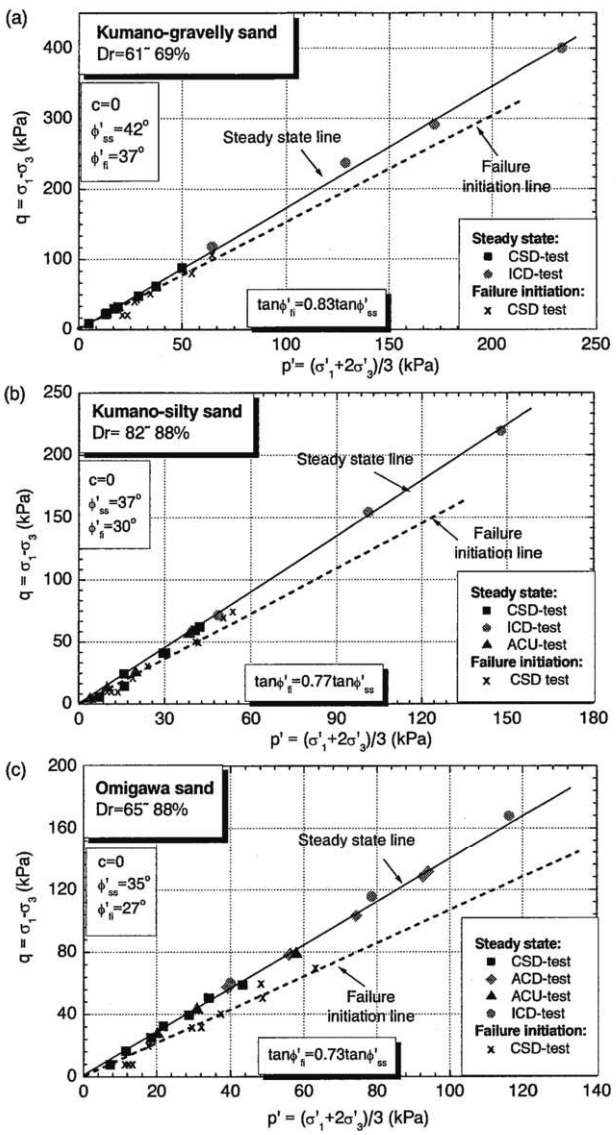

Figure 6. Plots of steady state conditions for all stress paths considered and failure initiation line in CSD tests: (a) Kumano-gravelly sand; (b) Kumano-silty sand; (c) Omigawa sand

REFERENCES

Anderson, S. A. and Sitar, N. (1995). Analysis of rainfall-induced debris flows. *Journal of Geotechnical Engineering, ASCE*, 121 (7), 544-552.

Brand, E.W. (1981). Some thoughts on rain-induced slope failures. *Proc., 10th ICSMFE*, Stockholm, 3, 373-376.

Brenner R.P., Tam, H.K. and Brand, E.W. (1985). Field stress path simulation of rain-induced slope failure. *Proc., 11th ICSMFE*, San Francisco, 2, 991-996.

Farooq, K. (2002). Experimental study on failure initiation in sandy slopes due to rainfall infiltration. *PhD Thesis*, University of Tokyo.

Fell, R., Hungr, O., Leroueil, S. and Reimer, W. (2000). Keynote lecture: Geotechnical engineering of the stability of natural slopes, and cuts and fills in soil. *Proc., GeoEng2000*, Melbourne, 1, 21-120.